Published by Avanti Publishers

Journal of Advances in Applied & Computational Mathematics

ISSN (online): 2409-5761

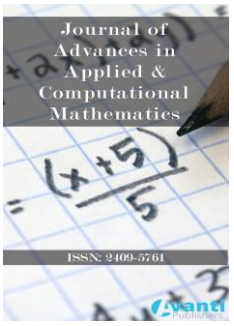

Numerical Investigation on Flow-Field Characteristics towards Removal of Free-Water by A Separator with Coalescing Plates

Xiangdong Qi[1], Hongqi Zhang[2], Xitong Sun[1,3] and Zhihua Wang[1,*]

[1]*Key Laboratory for Enhanced Oil & Gas Recovery of the Ministry of Education, Northeast Petroleum University, Daqing 163318, China*

[2]*Oil Recovery Plant No. 2, PetroChina Daqing Oilfield Company Limited, Daqing 163414, China*

[3]*Jilin Branch of China Aviation Fuel Company Limited, Changchun 130500, China*

ARTICLE INFO

Article Type: Research Article

Academic Editor: Riaz Ahmad Gill

Keywords:
Oil-water separation
Free-water knockout
Flow-field characteristics
Separation performance
Mathematical simulation

Timeline:
Received: March 10, 2023
Accepted: April 11, 2023
Published: May 10, 2023

Citation: Qi X, Zhang H, Sun X, Wang Z. Numerical investigation on flow-field characteristics towards removal of free-water by a separator with coalescing plates. J Adv App Comput Math. 2023; 10: 1-17.

DOI: https://doi.org/10.15377/2409-5761.2023.10.1

ABSTRACT

The produced water-containing polymer brings new challenges to oil-water separation in oilfield production, yet separators with coalescing plates to remove free water have been playing an active role. In this paper, the flow-field characteristics of polymer-laden produced water in a separator with coalescing plates are analyzed using computerized mathematical methods to investigate the effects with a water content of 55%, 70%, and 85%, flow rate of 3500 m^3/d, 4800 m^3/d, and 6000 m^3/d, and duration time of 20 min, 40 min, and 60 min on flow-field properties and separating efficiency are studied. The results show that the separating efficiency is positively correlated with water content and duration time, and duration time has the greatest improvement to the separating efficiency, but the enhancement of flow rate may reduce the separating efficiency. It is also observed that the separation efficiency of free-water reached 70.9% and the water content at the oil outlet of the separator reached 20.4% at a duration time of 60 min, when the contained polymer concentration and water content in the oil-water mixture are 500 mg/L and 70%, respectively.

*Corresponding Author
Email: zhihua_wang@126.com
Tel: +(86) 459 6503 102

1. Introduction

With the intensive exploitation of oilfields, a variety of measures such as water flooding and chemical agents have been widely used, thus crude oil production and economic benefits have been guaranteed [1-3]. Subsequently, the prevalence of impurities such as water, sediment, and polymers are commonly present in the produced water from oil wells, respectively, the transportation and utilization of crude oil are affected and threats to the environment may increase [4-5]. Furthermore, the oil-water interfacial stability is affected by components such as polymer and asphaltene in produced water, which brings new challenges to the treatment of produced water [5-7]. Typically, water and crude oil mixture need to be separated and treated in the oilfield to achieve compliance with refining and commercial requirements [8-10].

The existent form of water in crude oil is not fixed, so the difficulty of separation and treatment will continue to change. Free water is separated from oil in a short time by gravity sedimentation at room temperature, on the contrary, some amount of water will form a stable emulsion with crude oil, which is difficult to separate by gravity sedimentation [11, 12]. In industry, the process of separating free water and then treating oil-water emulsion has been applied on a certain scale [13]. Therefore, efficient separation of free water from emulsion is important.

Although free water is usually separated by gravity, there are differences in specific treatment equipment and methods [12-14]. At the same time, the separation effect will also change significantly. For example, wang *et al*. [15] simulated a separator with a bi-directional corrugated plate structure, which can obtain higher separating efficiency when the oil concentration is 30% to 60% and the flow rate of the inlet is 13 L/min ~ 133 L/min. Moreover, lower oil concentrations allow the selection of larger inlet flow rates within the appropriate range. Almarouf *et al*. [16] arranged a series of inclined multi-arc coalescing plates in the oil-water separator and proposed that the geometrical characteristics of the separator govern the separation effect between oil and water. Under the conditions of longer duration time and higher water content, the separation effect between oil and water will be enhanced, and the processing temperature and degree of oil shedding are linear. Kim *et al*. [17] simulated the influence of mesh size on the separation of an oil-water mixture under different pressure gradients, and the narrow pores can improve interfacial resistance and viscous dissipation, which help prevent oil infiltration by consuming oil inertia. From the point of coalescence and breakup of droplets, Yuan *et al*. [18] considered that droplets with smaller surface tension are suitable for lower separation speed, and separating efficiency can be enhanced by controlling the shape and spacing of wave plates, on the contrary, the speed of droplets with larger surface tension is a convenient way to increase the separating efficiency. Oruç *et al*. [19] experimentally studied the separating of mixtures at different temperatures, taking into account the corrugated plate spacing, shape, and angle, and obtained the highest value of separating efficiency. Yayla *et al*. [20, 21] investigated the influence of the Reynolds Number and the configuration of the coalescing plate on the oil-water separation. They found that the Reynolds Number of the oil-water mixture was inversely related to the separating efficiency. When the hole shape of the coalescing plate is elliptical and rectangular, the size of the hole does not affect separating efficiency. Moreover, when the distance of the coalescing plate is 12 mm and the Reynolds Number is 18, the separating efficiency is the highest for a cylinder with an aperture of 15 mm. In general, the various methods of removal of free water have the same goal, that is, by creating good conditions, oil and water rely on density difference and by the gravity to separate, and liquid separation plate and coalescing plate plays an irreplaceable role in this segment.

However, the properties of produced water are constantly changing when the polymer continues to exist, and the adaptability of the traditional separator to an oil-water mixture containing polymer is reduced, thus the separation effect of free-water has not reached the expected goal [13, 14, 22]. On the other hand, the separator with coalescing plates is widely used as the free-water separation equipment in oilfields, and the separation effect of oil-water mixtures containing polymers also lacks systematic evaluation.

Therefore, the suitability of oil-water mixtures containing polymers in separators with coalescing plates should be understood. The flow-field characteristics of the separation are concentrated reflections of the removal effect of free water, which is also inevitably affected by factors such as water content, flow rate, and duration time. Meanwhile, the separation effect of an oil-water mixture containing polymer in the separator provides a reference for the optimization of the separator structure.

In this paper, a Φ3600 mm×16000 mm separator with coalescing plates is built for mathematical simulation. The EULERIAN model and RNG *k-ε* model are applied to simulate the flow-field characteristics in the separator, and the role of steady flow and coalescence unit is shown. The separation of free water with the effect of water content, flow rate, and duration time of oil-water mixture containing polymer is studied by combining qualitative and quantitative methods. The flow-field change of the separator is further discussed by detecting the pressure field, flow field, and oil phase concentration distribution, furthermore, the oil-water separation effect is also evaluated.

2. Methodology

2.1. Modeling of Separator with Coalescing Plates

In the process of oil-water separation in Daqing Oilfield (China), a horizontal settling separator is mainly used to separate free water, and its model is Φ 3600 mm×16000 mm separator with coalescing plates, which has been widely used. Therefore, a physical model with an equal proportion to the separator is established.

The separation of oil and water depends on the steady flow unit and coalescence unit in the separator. As shown in Fig. (**1a**), the liquid separation plate is used as a steady flow unit, and the coalescing plate is used as a coalescence unit. The goal of oil-water separation can be achieved through these units. This is because the flow field becomes stable within the unit area, the oil droplets rise upward and the water phase settles downward.

Therefore, during the numerical simulation, the structure of the separator is reasonably simplified, the auxiliary components such as the oil tank and the base inside the separator are omitted, and the components such as the manhole and safety valve group outside the separator are not considered. As shown in Fig. (**1b**), a simplified physical model of the separator is constructed, and the coalescing plate is arranged horizontally. The main structural dimensions of the separator can be obtained from Table **1**.

Table 1: Structure size data of separator with coalescing plates.

Structural Parameters	Size	Structural Parameters	Size
Total volume of separator (m^3)	160	Oil phase outlet diameter (mm)	300
Length of elliptical heads at both ends of separator(mm)	500	Water phase outlet diameter (mm)	300
Total length of separator (mm)	16000	Distance from inlet to liquid separation plate (mm)	2100
Inlet diameter (mm)	300	Distance from inlet to the center of coalescing plate (mm)	9100
Length of coalescing plate (mm)	8000	Coalescing plate spacing (mm)	150
Thickness of liquid separation plate (mm)	20	Thickness of coalescing plate (mm)	20
Hole diameter of liquid separation plate (mm)	230	Opening ratio of liquid separation plate (%)	15

In the process of removing free water by using the separator, the oil-water mixture enters the inside of the separator in a tangential direction through the inlet, and the initial steady flow is realized by the liquid separation plate and then enters the coalescence unit. At this time, the lower density of the oil makes it rise and coalesce to the bottom surface of the coalescing plate, in turn, the higher density of the water makes it settle to the upper surface of the coalescing plate. The liquid in the coalescing plate will be continuously promoted from the entrance. Subsequently, the oil flows out from the oil outlet at the upper right end, and water flows out from the water outlet at the lower right end, and the separation of free water is realized.

2.2. Mathematical Model for Simulation of Coalescence-Separation

Before selecting the mathematical model, the temperature and pressure characteristics of the free-water separator are considered, and the energy exchange can be neglected.

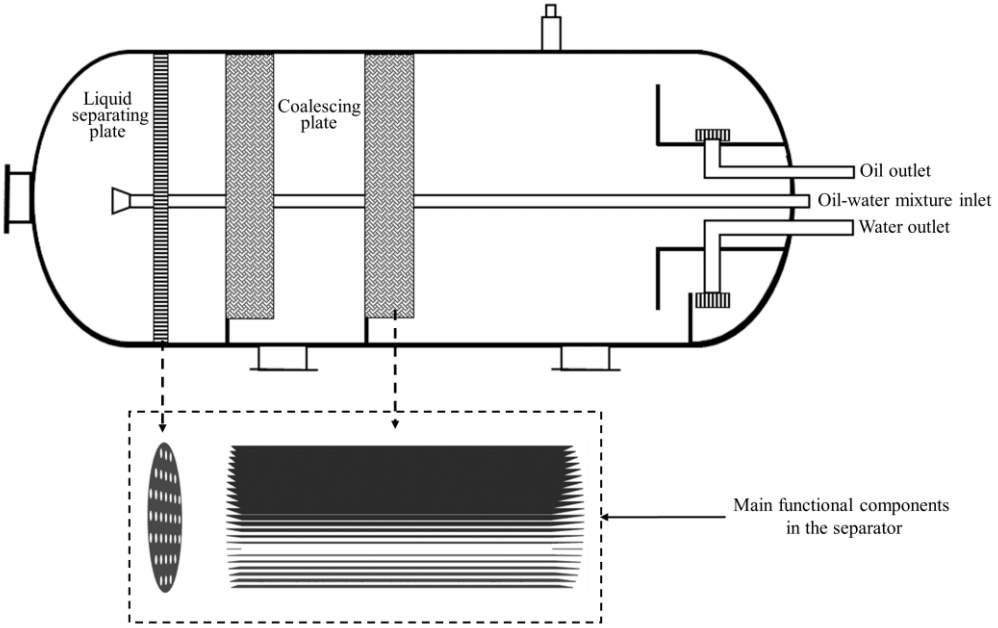

(a) Structure diagram of separator

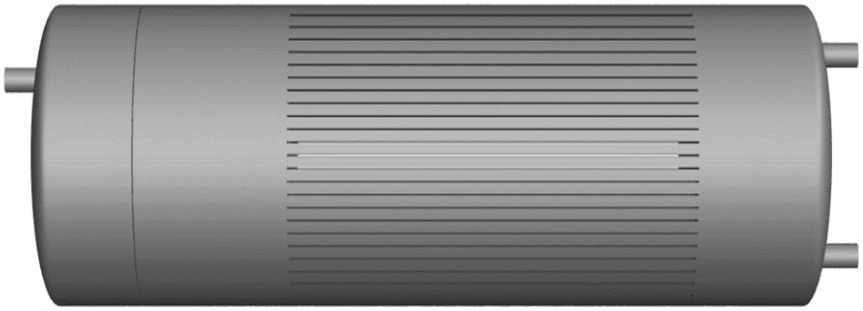

(b) Simplified physical model of separator

Figure 1: Main structure and modeling of Φ3600 mm×16000 mm separator with coalescing plates.

Continuity equation [23, 24]:

$$\frac{\partial(\rho u_x)}{\partial x}+\frac{\partial(\rho u_y)}{\partial y}+\frac{\partial(\rho u_z)}{\partial z}+\frac{\partial \rho}{\partial t}=0 \tag{1}$$

Momentum equation [25, 26]:

$$\begin{cases}\dfrac{\partial(\rho_m v_m)}{\partial t}+\nabla\,(\rho_m v_m v_m)=[\mu_m(\nabla v_m+\nabla_v^T)]+\nabla\,(\sum_{j=1}^{2}\alpha_j\rho_j v_{dr,j}^2)+\rho_m g+F-\nabla p \\ v_{dr,j}=v_j-v_m \\ \mu_m=\sum_{j=1}^{n}\alpha_j\mu_j \\ \nabla p=\dfrac{\partial p}{\partial x}+\dfrac{\partial p}{\partial y}+\dfrac{\partial p}{\partial z}\end{cases} \tag{2}$$

where $\rho_m$is the density of the oil-water mixture, kg/m^3; v_m is the mass average velocity of the oil-water mixture, m/s; μ_m is the dynamic viscosity of the mixture, Pa·s; α_j is the volume fraction of phase *j*, %; ρ_j is the density of

phase j, kg/m^3; $v_{dr,j}$ is the drift velocity of phase j, m/s; F is the external force, N; v_j is the mass velocity of phase j, m/s; μ_j is the dynamic viscosity of phase j, Pa·s ; p is the pressure shared by all phases, Pa.

The equation for the volume fraction of the oil phase can be derived from the continuity equation as follows:

$$\frac{\partial(\alpha_k\rho_k)}{\partial t} + \nabla\ (\alpha_k\rho_k v_m) + \nabla(\alpha_k\rho_k v_{dr,k}) = 0 \tag{3}$$

Where $v_{dr,k}$is the drift velocity of phase *k*, m/s; α_k is the volume fraction of phase *k*, %; ρ_k is the density of phase *k*, kg/m^3."

In the simulation of oil-water separating, the flow pattern of the oil-water mixture in the separator should be determined before simulation. The identification of the flow pattern can be quantitatively distinguished by the Reynolds Number. Laminar flow has a small Reynolds Number and high viscous forces in the flow field. In contrast, the turbulent flow has a large Reynolds Number, high inertial forces in the flow field, an extremely unstable flow state, and a relatively disordered flow field [27, 28].

Reynolds Number can determine the flow state of the oil-water mixture in the separator, which can be obtained from Eq. (4) [25, 29].

$$Re = \frac{\rho_m v d_c}{\mu} \tag{4}$$

Where $Re$is the Reynolds Number of the oil-water mixture in the separator; ρ_m is the density of the mixture, kg/m^3; v is the average velocity of the mixture in the separator, m/s; d_c is the equivalent diameter of separator, mm; μ is the dynamic viscosity of mixture in the separator, Pa·s.

The density of the oil-water mixture can be calculated according to Eq. (5).

$$\rho_m = \rho_o(1-\psi) + \rho_w\psi \tag{5}$$

Where $\rho_o$is the density of oil, kg/m^3; ρ_w is the density of water, kg/m^3; ψ is the water content of the mixture, %.

The basic structural characteristics of separators with coalescing plates are considered. Reynolds Number is calculated by Eq. (4) and (5), then the flow pattern is identified. After the analysis and calculation of the working conditions of a treatment station in an oilfield, the free-water separation process is defined as a turbulent flow pattern. Therefore, the widely used and applicable RNG *k-ε* model is used for simulation [30, 31].

Moreover, oil and water phase volume fractions are extracted to quantitatively characterize the oil-water separation effect after the calculation runs stably, and the free-water separation efficiency of the oil-water mixture in the separator can be calculated according to Eq. (6).

$$\eta = \frac{\varphi_1 - \varphi_2}{\varphi_1} \tag{6}$$

where $\eta$is the separation efficiency of free-water, %; φ_1 is water phase volume fraction at the inlet, %; φ_2 is water phase volume fraction at the oil outlet, %.

2.3. Solving Process

Based on the established physical model of the separator, the finite volume method is used to solve it, dividing the calculation area of the physical model into non-repeating control volumes (grids), integrating the conservation-type differential equations to be solved in any control volume and a certain time interval over space and time, and specifically completing the application of the algorithm in the model by the commercial software FLUENT.

The grid type is generally divided into structured grid and unstructured grid. Among them, the unstructured grid has good adaptability to complex models [32]. Fluent Meshing is used to generate an unstructured grid after

the structure of the separator is considered. Since the liquid separation plate and the coalescing plate are the main implementation areas of the separation function, they are reasonably encrypted. In addition, grid independence verification is accomplished by encrypting the number of grids in the computational domain, and the separator outlet velocity variation is observed at different grid numbers. The relative error of the simulation results decreases with increasing the number of grids, and the grid convergence can be considered when the error is lower than 5%, and finally, the physical model with the grid number 5086345 is used for the formal simulation calculation, and the meshing of the separator is shown in Fig. (**2**).

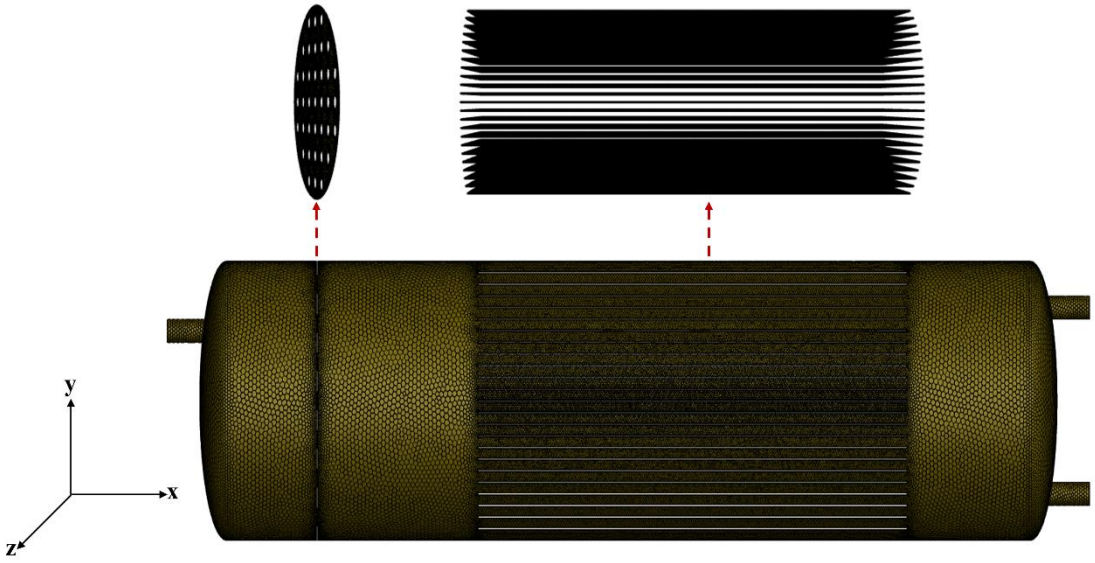

Figure 2: Meshing of Φ3600 mm×16000 mm separator with coalescing plates.

In the FLUENT software, the wall is set to a static state by considering the influence of the viscosity of the wall of the separator. After a given inlet velocity, the outlet boundary of both water and oil is set to “Outflow". Similarly, the steady flow unit and coalescence unit play an important role. For a clearer understanding of the separation effect and obtaining the separation flow-field characteristics inside the separator, the mixture composed of oil and water is considered to be incompressible fluids in the simulation process. The temperature inside the separator has been kept constant so that heat exchange has been ignored.

The parameters selected for the simulation calculations are determined according to the physical properties of the oil-water mixture in the Daqing oilfield, as shown in Table **2**. Due to the mutual motion between the oil and water phases, a non-constant calculation of the simulation process is chosen for “Phase Coupled Simple” [33].

Table 2: Basic calculation parameters of oil - water separation simulation.

Calculation Parameters	Value
Concentration of polymer in oil-water mixture (mg/L)	500
Water phase density (kg/m^3)	1000
Oil phase density (kg/m^3)	845
Oil phase viscosity (mPa·s)	56
Oil-water interfacial tension (N/m)	0.03
Separation temperature (°C)	38
Initial height of oil-water interface (m)	2.5
Contact angle of upper surface of coalescing plate (°)	20
Contact angle of lower surface of coalescing plate (°)	150

3. Results and Discussion

In the operation of a separator, the separation flow field characteristics can be represented by pressure, velocity, streamline, and volume fraction of the phase [15, 17, 21]. Thus, the distribution characteristics of the pressure field, velocity field, and concentration field, as well as the streamlined distribution characteristics inside the separator are observed and analyzed, and the oil-water separation effect of the separator is evaluated. Furthermore, the water content and flow rate are selected based on the nature of the oil-water mixture provided by Daqing Oilfield, while the duration time of the oil-water mixture in the separator is determined by actual process experience. For better quantitative analysis, pressure, and oil phase volume distributions are observed on the separator z=0 profile, and correlation data are extracted parallel to the separator profile and every 0.1 m in the Y direction under conditions relative to the outlet boundary.

3.1. Flow-Field Characteristics of the Separator

Oil-water mixture with a water content of 70%, containing a polymer concentration of 500 mg/L, and a flow rate of 4800 m^3/d is selected as a case after the physical properties of the produced water are analyzed. The flow-field characteristics of oil-water separation are further revealed by calculation results. The important role of the stability of the working pressure inside the separator on the separation performance is considered, and the distribution of the pressure field in the separator is shown in Fig. (**3a**). The uniform decrease of the pressure distribution in the separator from bottom to top can be observed, and the maximum pressure difference is about 3.3 kPa, which confirms separator has good operation stability.

As shown in Fig. (**3b**), velocity vector distribution in the separator is extracted, and the flow-field distribution during the separation process is more intuitively reflected. The oil-water mixture enters the interior from the left inlet of the separator, and the flow field of the separator is impacted by the maximum flow rate. However, the distribution of the flow rate change uniformly after passing through the steady flow of the liquid-separating plate. Meanwhile, the flow field in the separator tends to be stable, and the role of the liquid separation plate as a steady flow unit is demonstrated.

Fig. (**3c**) shows the streamlined distribution characteristics inside the separator. Similarly, the streamline is the most intuitive manifestation of separation flow-field characteristics during the separation of free water. It can be found that the high flow rate of the inlet brings significant disturbance to the streamline in the inlet area, and the chaotic state of the streamline can be observed. However, the streamline distribution tends to be stable as a whole, after passing through the coalescence area.

The separating effect of the separator is shown in Fig. (**3d**), and the change in the volume fraction of oil is the main manifestation. The stratification of the oil/water interface inside the separator exists, however, the stratification of the oil and water interface is more chaotic before entering the coalescence area. The stratification of the oil/water interface is transformed into a clear form after passing through the coalescing plate, the higher oil phase volume fraction area is thickened, and the lower oil phase volume fraction area is continuously thinned.

3.2. Effect of Water Content on Flow-Field Characteristics

The interfering factors of the flow-field characteristics and separation effect in the separator are taken as research objectives. Initially, the effect of water content is explored based on flow-field characteristics in the separator, and the control variable method is used, that is, the contained polymer concentration and flow rate of the oil-water mixture remain unchanged. Then, three kinds of oil-water mixture with a water content of 55%, 70%, and 85% are simulated and analyzed after the production, and research data are referred to.

3.2.1. Pressure Field Distribution and Pressure Drop Characteristics

Pressure field distribution in the separator is compared and analyzed in Fig. (**4**). The pressure field distribution of the mixture under the three kinds of water content is the same during the separation process, respectively, when the contained polymer concentration and flow rate are 500 mg/L and 4800 m^3/d. The pressure drop of the

cross-section increases slightly, and pressure field distribution in the separator is generally stable as the water content of the mixture increases from 55% to 85%.

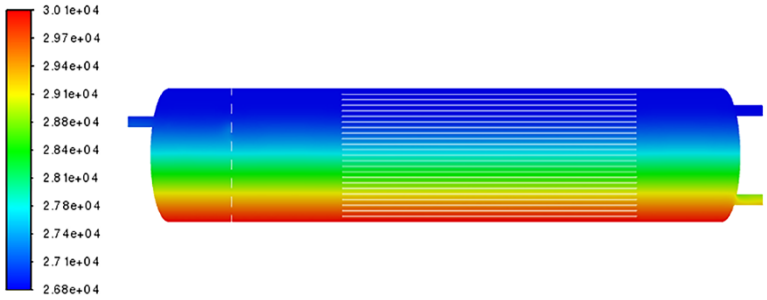

(a) Pressure distribution

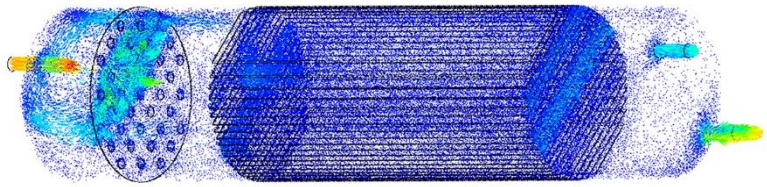

(b) Velocity vector distribution

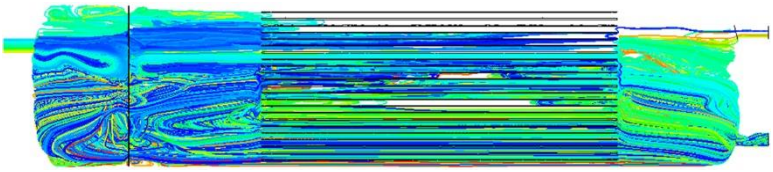

(c) Streamline distribution

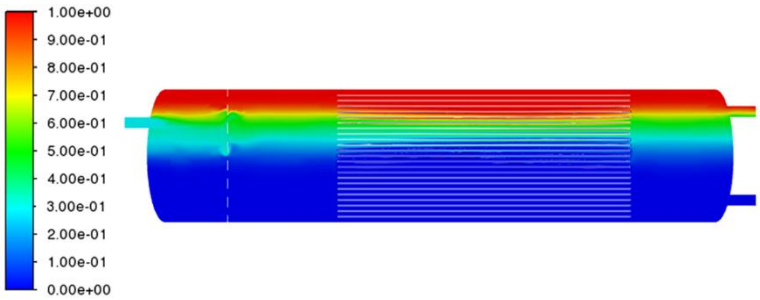

(d) Distribution of oil phase volume fraction

Figure 3: Flow-field characteristics in separator with the water content of 70%, the contained polymer concentration of 500 mg/L, and the flow rate of 4800 m^3/d.

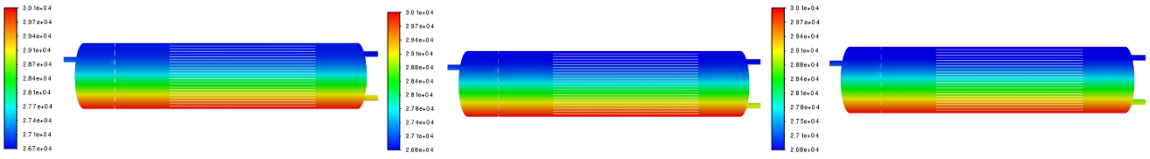

(a) 55% **(b) 70%** **(c) 85%**

Figure 4: Pressure distribution in separator with water content of 55%, 70% and 80%. (z=0)

As shown in Fig. (**5**), pressure field distribution of the e-separation process is further quantitatively described, and then the characteristic of pressure drop is drawn. The pressure drop changes of the free-water separation process with different water content are similar, and the average increase of pressure drop is 4.80%, respectively, when the water content increases from 55% to 85%.

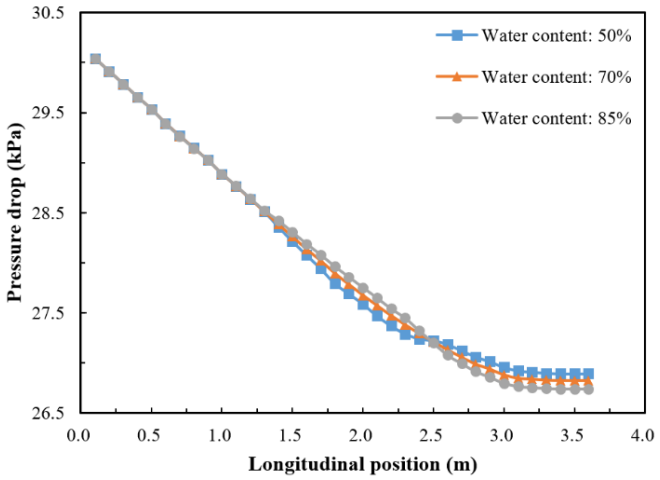

Figure 5: Characteristics of pressure drop in separator with water content of 55%, 70% and 80%.

3.2.2. Streamline Distribution Characteristics

As shown in Fig. (**6**), the streamlined distribution of an oil-water mixture with three kinds of water content in a separator with coalescing plates is shown. There is a ' gap ' in the streamlining of the oil-water mixture with 55% water content during the separation process, respectively, the stability of the internal flow field of the separator may be reduced. The dispersion performance of the fluid is more significant when the water content increases from 55% to 70% and 85%, and the phenomenon is consistent with the reduction of interphase stability caused by higher water content.

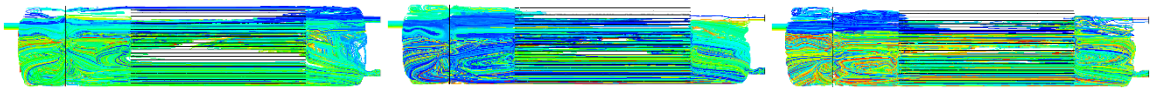

(a) 55% **(b) 70%** **(c) 85%**

Figure 6: Streamline distribution in separator with water content of 55%, 70% and 80%. (z=0).

3.2.3. Oil Phase Concentration Distribution Characteristics

As shown in Fig. (**7**) and Fig. (**8**), the oil/water interface characteristics of the mixture with different water contents in the separator are compared and analyzed, and the oil volume fraction is extracted. The oil-water interface stratification changes to fuzzy with the increase in water content. Overall, the distribution of the oil phase volume ratio in the separator is more regular. The maximum and minimum values of the oil phase volume ratio are obtained when the water content is 85% and 55%, respectively, when the longitudinal position is below

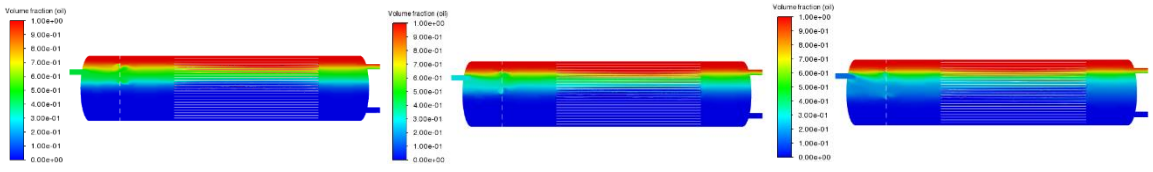

(a) 55% **(b) 70%** **(c) 85%**

Figure 7: Distribution of oil phase volume fraction in separator with water content of 55%, 70% and 80%. (z=0).

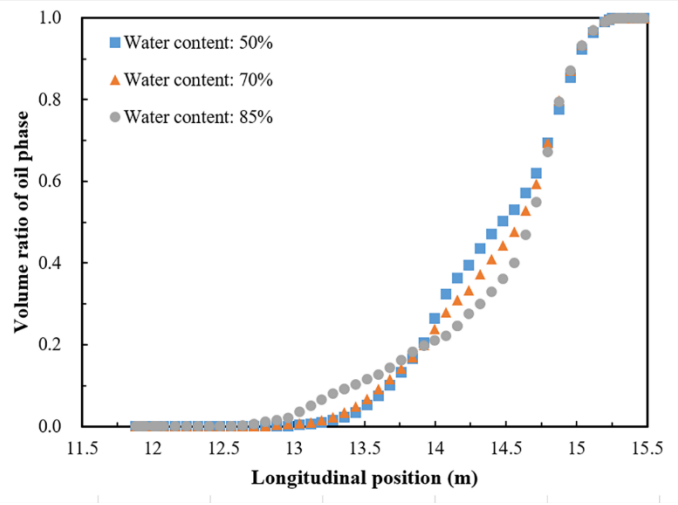

Figure 8: The volume ratio of oil phase in separator with water +content of 55%, 70% and 80%.

2m. On the contrary, the maximum and minimum values of the oil phase volume ratio are obtained when the water content is 55% and 85%, respectively, when the longitudinal position is in the range of 2m and 3m. However, the oil phase volume ratio after separation with a water content of 85% is higher than that with a water content of 55% and 70%, respectively, when the longitudinal position is above 3m.

3.3. Effect of Flow Rate on Flow-Field Characteristics

The effect of flow rate on the flow-field characteristics and separating efficiency is studied, and the pressure field, streamline, and oil phase volume fraction distribution are also analyzed. Similarly, the contained polymer concentration and water content of the mixture are kept at 500 mg/L and 70%, respectively, when flow rates of 3500 m^3/d, 4800 m^3/d, and 6000 m^3/d are simulated and analyzed.

3.3.1. Pressure Field Distribution and Pressure Drop Characteristics

As shown in Fig. (**9**), the distribution of the pressure field in the separator is extracted with different flow rates. The pressure field in the mixture separating is the same, and the pressure field distribution in the separator is steady, but the pressure drop decreases slightly with the enhancement of the flow rate. Further, pressure field distribution in the separation process of free water affected by flow rate is quantitatively described. The characteristic of pressure drop in the separator is shown in Fig. (**10**), and pressure drop changes of the three kinds of flow rate are coincident. The steady state of the pressure change characteristics during the operation of a separator with coalescing plates is displayed, and the fluctuation of the flow rate does not bring a significant impact on the pressure field in the separator.

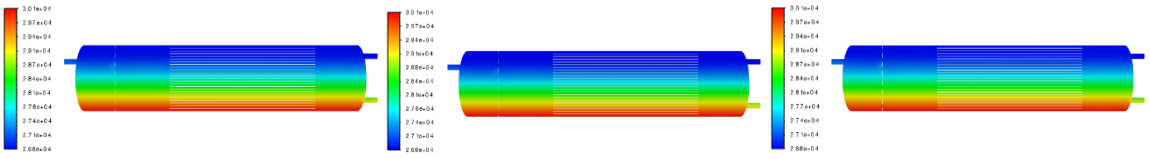

(a) 3500 m^3/d **(b) 4800 m^3/d** **(c) 6000 m^3/d**

Figure 9: Pressure distribution in separator with flow rate of 3500 m^3/d, 4800 m^3/d and 6000 m^3/d. (z=0).

3.3.2. Streamline Distribution Characteristics

As shown in Fig. (**11**), the flow field in the separator is displayed from another perspective, and the streamline in the separator with the flow rate of 3500 m^3/d, 4800 m^3/d, and 6000 m^3/d are analyzed, respectively, when the contained polymer concentration and water content of the oil-water mixture are 500 mg/L and 70%. There are many ' gaps ' between +-the streamlines in the separated flow field when the flow rate is 3500m^3/d. The ' gap ' in

the separator is filled, and the phenomenon of eddy current begins to appear and developed, respectively, when the flow rate increased from 3500 m^3/d to 4800 m^3/d and 6000 m^3/d. Eventually, it can be observed in Fig. (**11c**) that the flow field is no longer smooth.

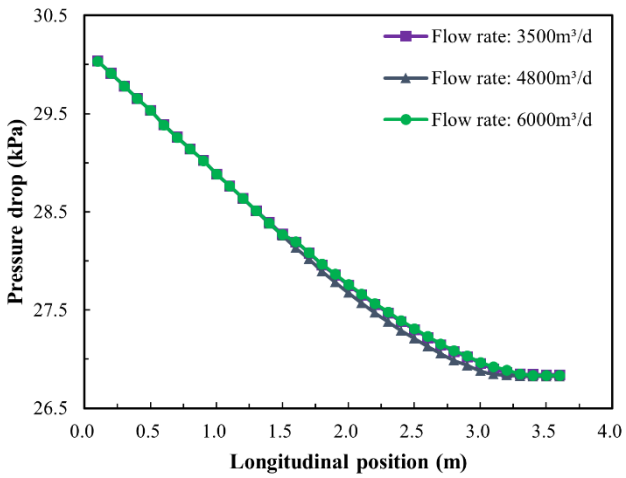

Figure 10: Characteristics of pressure drop in separator with flow rate of 3500 m^3/d, 4800 m^3/d and 6000 m^3/d.

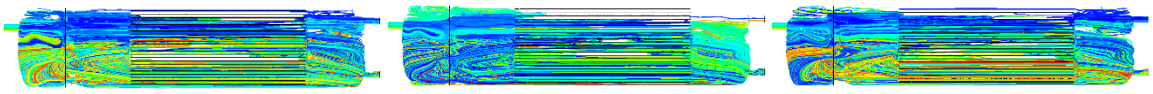

(a) 3500 m^3/d **(b) 4800 m^3/d** **(c) 6000 m^3/d**

Figure 11: Streamline distribution in separator with flow rate of 3500 m^3/d, 4800 m^3/d and 6000 m^3/d. (z=0).

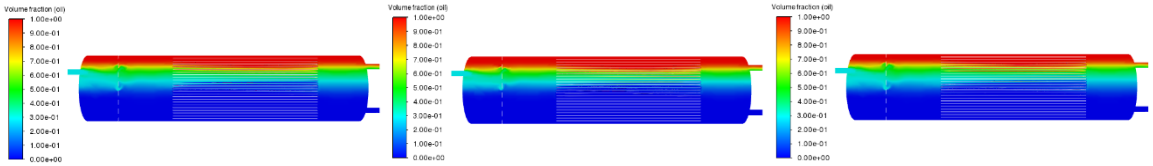

(a) 3500 m^3/d **(b) 4800 m^3/d** **(c) 6000 m^3/d**

Figure 12: Distribution of oil phase volume fraction in separator with flow rate of 3500 m^3/d, 4800 m^3/d and 6000 m^3/d. (z=0).

3.3.3. Oil Phase Concentration Distribution Characteristics

As shown in Fig. (**12**), Oil phase concentration distribution in the separator under the effect of different flow rates is obtained, and the oil/water interface state and variation characteristics in the separator are observed. Overall, the oil/water interface in the separator is relatively flat with different flow rates. Higher oil phase concentration distribution gradually becomes thicker, and lower oil phase concentration distribution gradually becomes thinner, respectively, when the flow rate enhances from 3500 m^3/d to 4800 m^3/d. The difference is that higher oil phase concentration distribution becomes thinner and lower oil phase concentration distribution becomes thicker, respectively, when the flow rate increases from 4800 m^3/d to 6000 m^3/d, in addition, the change of oil phase concentration distribution is affected by streamlined distribution characteristics is further verified.

As shown in Fig. (**13**), the volume ratio of oil in an e-separator with different flow rates is extracted for quantitative analysis. The volume ratio of oil is the highest for a flow rate is 6000 m^3/d, and the smallest for a flow rate is 4800 m^3/d, respectively, when the longitudinal position of the separator is below 2.4 m. However, the volume ratio of the oil phase is the highest for a flow rate is 4800 m^3/d for the separator longitudinal position above 2.4 m.

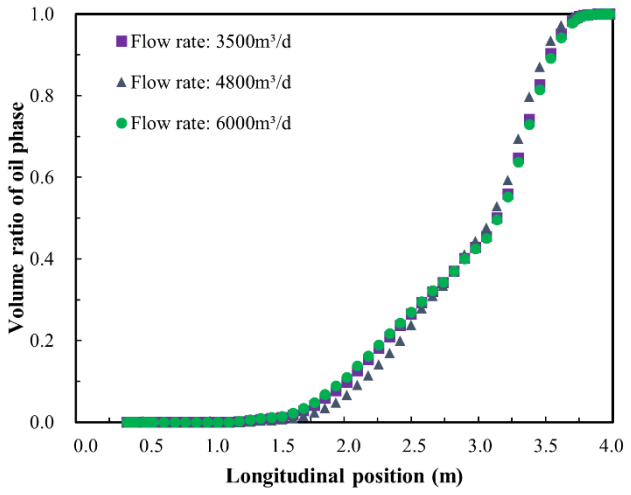

Figure 13: The volume ratio of oil phase in separator with flow rate of 3500 m^3/d, 4800 m^3/d and 6000 m^3/d.

3.4. Effect of Duration Time on Flow-Field Characteristics

Eventually, the influence of duration time on the separation flow-field characteristics and separation effect is studied after understanding the effect of water content and flow rate. The duration time of the oil-water mixture in the separator is changed when the contained polymer concentration and water content of the oil-water mixture are 500 mg/L and 70%. In this study, three kinds of duration time about 20 min, 40 min, and 60 min are simulated and selected.

3.4.1. Pressure Field Distribution and Pressure Drop Characteristics

As shown in Fig. (**14**), there is a significant difference in the distribution of the pressure field in the separator when the duration time chosen is 20 min, 40 min, and 60 min. The pressure drop in the separator increases with the extension of the duration time, and pressure loss is reduced, which may be due to the reduction of the flow rate in unit time, and the longer duration time makes the pressure drop in the separator increase.

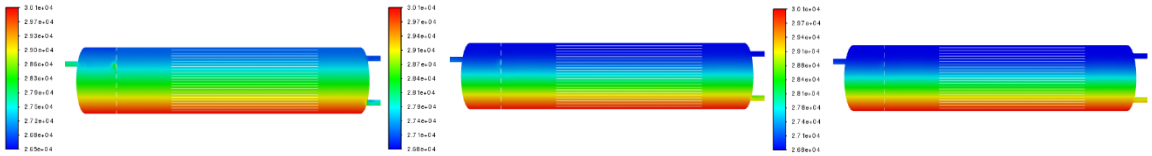

(a) 20 min **(b) 40 min** **(c) 60 min**

Figure 14: Pressure distribution in separator with duration time of 20 min, 40 min and 60 min. (z=0).

As shown in Fig. (**15**), the pressure field distribution of the free-water separating process in the separator is quantitatively described by the pressure drop characteristic. The pressure drop increases significantly after 60 min duration time, respectively, when the vertical position of the separator is above 1m and compared with other duration times, and the consistency of pressure distribution and pressure drop characteristics is confirmed.

3.4.2. Streamline Distribution Characteristics

As shown in Fig. (**16**), the streamlined characteristics of the oil-water mixture in a separator with coalescing plates are similar, respectively, when the duration time is 20 min, 40 min, and 60 min. However, there are obvious phenomena of ' eddy current 'in many places in the separator, when the duration time is 20 min. In Fig. (**16c**), the phenomenon of ' eddy current ' is greatly reduced, and the stability of the separation flow field is continuously improved for a duration time of 60 min. The separation effect of free water can be improved with an extension of duration time.

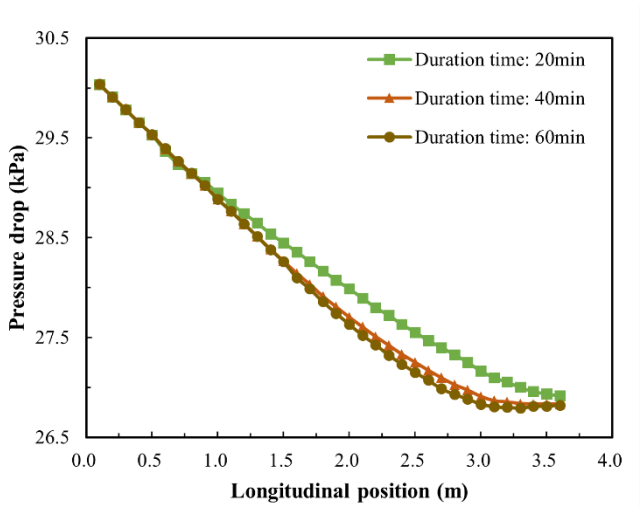

Figure 15: Characteristics of pressure drop in separator with duration time of 20 min, 40 min and 60 min.

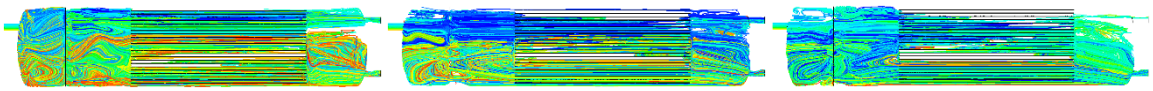

(a) 20 min **(b) 40 min** **(c) 60 min**

Figure 16: Streamline distribution in separator with duration time of 20 min, 40 min and 60 min. (z=0)

3.4.3. Oil Phase Concentration Distribution Characteristics

As shown in Fig. (**17**), there are obvious differences in the distribution of oil phase volume in the separator with the influence of duration time. The oil/water interface in Fig. (**17a**) is irregular when the duration time is 20 min. After the duration time is extended, the oil/water interface changes from chaos to clarity, and the oil-water stratification becomes more and more obvious, respectively, and the concentration distribution areas of higher and lower oil phases become thicker and thinner.

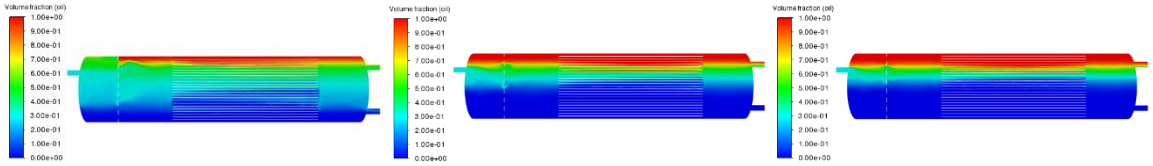

(a) 20 min **(b) 40 min** **(c) 60 min**

Figure 17: Distribution of oil phase volume fraction in separator with duration time of 20 min, 40 min and 60 min. (z=0).

As shown in Fig. (**18**), the oil phase volume proportion in the separator with a duration time of 40 min and 60 min is relatively regular. The proportion with a duration time of 40 min is higher than that with a duration time of 60 min for a vertical position of the separator is below 2.4 m. On the contrary, the volume fraction is the highest when the duration time is 60 min for the area with a longitudinal position of more than 2.4 m. In contrast, the volume proportion in the upper half and lower half of the separator is low and high, respectively, when the duration time is 20 min. It is further proved that extending the duration time can promote the effect of oil and water separation.

3.5. Oil-Water Separation Performance

Oil-water separation is the ultimate goal of the separator, and the quality of the oil phase in the oil outlet should be guaranteed. The water content in oil should be lower than the specified value of the process flow and

the water content of the oil outlet should not exceed 30% [22, 34]. Therefore, the effects of water content, flow rate, and duration time on the separation of free water by a separator with coalescing plates are quantitatively characterized, respectively, and the volume fractions of oil and water are extracted. As shown in Fig. (**19**), the separating performance is mainly reflected by the water content of the oil outlet and the removal rate of free water, and the oil-water separation effect under different water content, flow rate, and duration time is compared and analyzed.

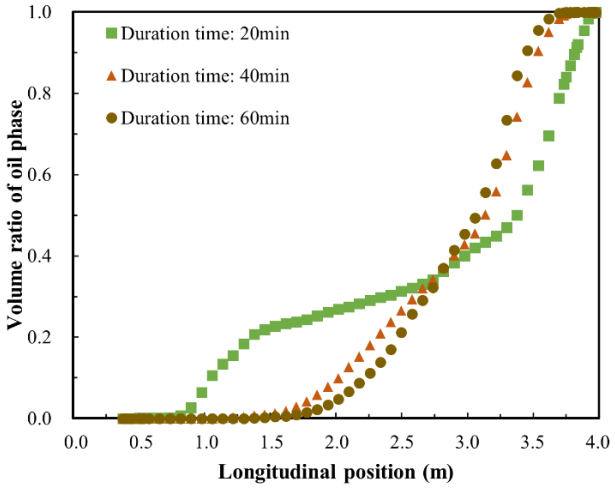

Figure 18: The volume ratio of oil phase in separator with duration time of 20 min, 40 min and 60 min.

As shown in Fig. (**19a**), the water content of the oil outlet increases when the water content of the mixture in the separator increases, respectively, the contained polymer concentration and flow rate are 500 mg/L and 4800 m^3/d. However, the rise in water content in oil outlets is not significant, although water content has always met the technical requirements of 30%. The water content of the oil outlet decreases when the flow rate increases from 3500 m^3/d to 4800 m^3/d, and the water content of the oil outlet increase when the flow rate continues to increase to 6000 m^3/d, respectively, when the contained polymer concentration and water content of 500 mg/L and 70%. In the separation simulation of a mixture with 30% oil content, the water content of the oil outlet also decreases first and then increases after changing the inlet flow rate, which is consistent with the simulation results of this paper [15]. Although the water content of the oil outlet is lower than the technical index of 30% required by the process, the irregularity of the water content of the oil outlet cannot be ignored, and separating performance should be evaluated in combination with the removal effect of free water. The water content at the oil outlet decreases from 45.4% to 20.4% when the duration time is extended from 20min to 60min, respectively, when the contained polymer concentration and water content of 500 mg/L and 70%. The increase in duration time not only makes the water content of the oil outlet meet the requirements for dehydration, but also significantly improves the oil phase concentration of the oil outlet, and the important role of duration time is further demonstrated. The result is consistent with the description of flow-field and oil phase volume fraction distribution.

The volume fraction of water and oil extracted after the calculation is stable, and the separation efficiency of free water in the separator is calculated by Eq. (6), and the separating effect is further quantitatively characterized. As shown in Fig. (**19b**), the separation efficiency of free-water increased from 54.7% to 68.8% with the water content in the oil-water mixture increased, respectively, when the contained polymer concentration and flow rate are 500 mg/L and 4800 m^3/d, but the increasing rate is decreased with the water content in the mixture increases. The separation efficiency of free water increased from 58.7% to 65.3% when the flow rate increased from 3500 m^3/d to 4800 m^3/d, respectively, when the contained polymer concentration and flow rate are 500 mg/L and 4800 m^3/d. The separation efficiency of free water decreased from 65.3% to 58.9% when the flow rate continued to increase to 6000 m^3/d. The separation efficiency is consistent with the qualitative description of flow-field and oil phase concentration distribution. The separating efficiency of free water increased from 35.1% to 70.9% when the duration time is extended from 20 min to 60 min, respectively, when the contained polymer concentration and flow rate are 500 mg/L and 4800 m^3/d. The separation efficiency of free water and the water content of the oil outlet confirm the important effect of duration time on oil-water separation.

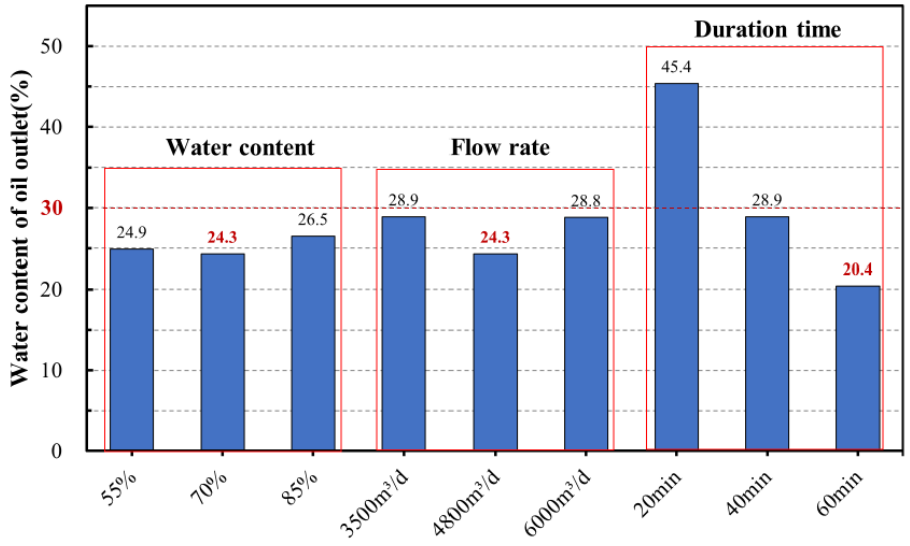

(a) Water content of oil outlet with different water content, flow rate and duration time.

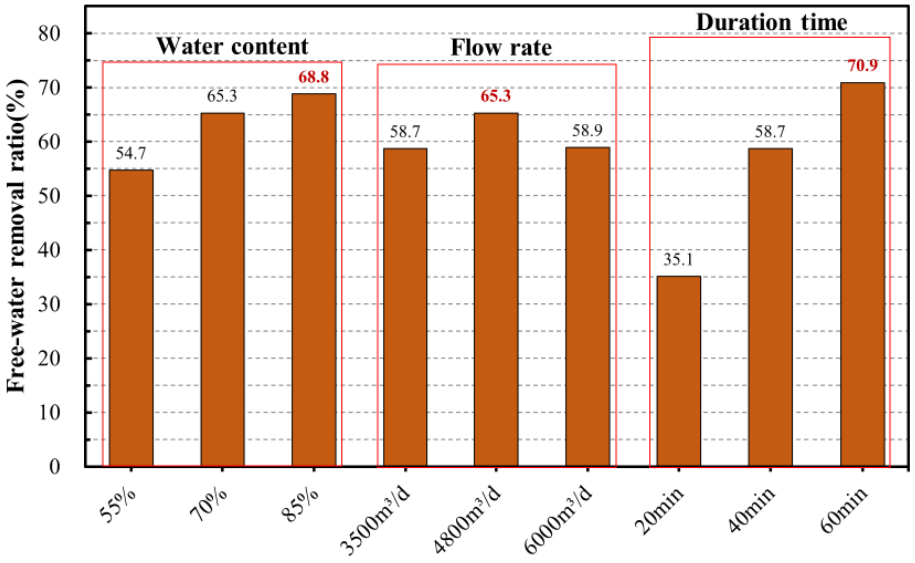

(b) Free-water removal ratio with different water content, flow rate and duration time.

Figure 19: Oil-water separation effect with different water content, flow rate and duration time.

The research of Almarouf *et al*. [16] and Yayla *et al*. [21] is consistent with the numerical simulated results in this paper. The separating efficiency of free water is positively correlated with the water content and duration time of the oil-water mixture, respectively, when the characteristics of the mixture and the specifications of the separator are similar.

4. Conclusion

The pressure, flow rate, and streamlined distribution of the oil-water mixture in a separator with coalescing plates reflect the important role of the steady flow and coalescence unit in building a stable flow field. The variation of oil phase volume fraction further confirms the oil-water separation performance of a separator with coalescing plates. In the separator, the separation efficiency of free water is positively correlated with the water content and duration time, and the effect of duration time was greater than that of water content and flow rate. When the duration time was 60 min, the water content at the oil outlet decreased to 20% and the separation efficiency of free water increased by about 71%. However, as the flow rate increased, the free-water separation

efficiency first increased and then decreased. When the contained polymer concentration in the oil-water mixture is 500 mg/L and the water content is 70%, the flow rate of the free-water separation process should be no higher than 6000 m^3/d.

Using mathematical methods to observe the flow-field characteristics of the oil-water mixture containing polymer in the separator can reveal the principle of action of a separator with coalescing plates, determine the influencing factors of the oil-water separation efficiency, and then improve the treatment methods and equipment parameters of the actual process to achieve efficient operation of oil-water separation. However, the variations of flow lines and oil phase volume fractions indicate that a separator with coalescing plates is not suitable for treating oil-water mixtures with higher water content. In addition, a separator with coalescing plates needs a suitable flow rate to ensure separation efficiency, which means that the separator with agglomerated plates cannot meet the demand of some high-speed production. Therefore, the structure of the coalescing plate separator can be optimized, and thus the separation efficiency of free water can be improved.

Acknowledgements

The research of this paper was supported by the National Natural Science Foundation of China (Grant No. 52074090; 52174060) and the Key Research & Development Program of Heilongjiang Province (Grant No. JD22A004). The authors also acknowledge the support of the Heilongjiang Touyan Innovation Team Program.

References

[1] Yuan S, Wang Q. New progress and prospect of oilfields development technologies in China. Pet Explor Dev. 2018; 45: 698-711. https://doi.org/10.1016/S1876-3804(18)30073-9

[2] Chaturvedi KR, Sharma T. Modified smart water flooding for promoting carbon dioxide utilization in shale enriched heterogeneous sandstone under surface conditions for oil recovery and storage prospects. Environ Sci Pollut R. 2022; 29: 41788-803. https://doi.org/10.1007/s11356-022-18851-6

[3] Gbadamosi A, Patil S, Kamal MS, Adewunmi AA, Yusuff AS, Agi A, *et al*. Application of polymers for chemical enhanced oil recovery: a review. Polymers. 2022; 14(7): 1433. https://doi.org/10.3390/polym14071433

[4] Tang N, Luo R, Xiao Y, Wanyan Q, Li K XJ, Zhang L, *et al*. Settlement experiment on insoluble particles in rock salt. Oil Gas Stor Trans. 2020; 39: 1136-41. https://doi.org/10.6047/j.issn.1000-8241.2020.10.008

[5] Zhang D, Chen Z, Ren L, Meng X, Gu W. Study on stability of produced water in ASP flooding based on critical micellar theory. Polym Bull. 2022; 79: 179-92. https://doi.org/10.1007/s00289-020-03497-6

[6] Xu Y, Wang H, Wang Z, Xu Z, Hong J, Sun W. Microscopic mechanism of asphaltene and resin behavior to the stability of oil-water interface. J North Petrol Univ. 2021; 45: 90-101. https://doi.org/10.3969/j.issn.2095-4107.2021.06.008

[7] Wang Z, Xu Y, Gan Y, Han X, Liu W, Xin H. Micromechanism of partially hydrolyzed polyacrylamide molecule agglomeration morphology and its impact on the stability of crude oil−water interfacial film. J Petrol Sci Eng. 2022; 214: 110492. https://doi.org/10.1016/j.petrol.2022.110492

[8] Pramadika H, Wastu ARR, Satiyawira B, Rosyidan C, Maulani M, Prima A, *et al*. Demulsification optimization process on separation of water with heavy oil. AIP Conference Proceedings 23 November 2021; 2363(1): 020029. https://doi.org/10.1063/5.0061527

[9] Zhu C, Liu X, Xu Y, Liu W, Wang Z. Determination of boundary temperature and intelligent control scheme for heavy oil field gathering and transportation system. J Pipeline Sci Eng. 2021; 1: 407-18. https://doi.org/10.1016/j.jpse.2021.09.007

[10] Xing L, Jiang M, Zhao L, Gao J, Liu L. Design and analysis of de-oiling coalescence hydrocyclone. Sep Sci Technol. 2022; 57: 749-67. https://doi.org/10.1080/01496395.2021.1945102

[11] Luo H, Wen J, Lv C, Wang Z. Modeling of viscosity of unstable crude oil–water mixture by characterization of energy consumption and crude oil physical properties. J Petrol Sci Eng. 2022; 212: 110222. https://doi.org/10.1016/j.petrol.2022.110222

[12] Mohayeji M, Farsi M, Rahimpour MR, Shariati A. Modeling and operability analysis of water separation from crude oil in an industrial gravitational coalescer. J Taiwan Inst Chem E. 2016; 60: 76-82. https://doi.org/10.1016/j.jtice.2015.10.025

[13] Amakiri KT, Canon AR, Molinari M, Angelis-Dimakis A. Review of oilfield produced water treatment technologies. Chemosphere. 2022; 298: 134064. https://doi.org/10.1016/j.chemosphere.2022.134064

[14] Han Y, He L, Luo X, Lü Y, Shi K, Chen J, *et al*. A review of the recent advances in design of corrugated plate packs applied for oil–water separation. J Ind Eng Chem. 2017; 53: 37-50. https://doi.org/10.1016/j.jiec.2017.04.029

[15] Wang X, Yan Y, Xu Z. Application experiment and numerical simulation analysis of oil–water separator with two-oriented corrugated coalescence plate. J Disp Sci Technol. 2017; 38: 1509-15. https://doi.org/10.1080/01932691.2016.1259072

[16] Almarouf HS, Nasser MS, Al-Marri MJ, Khraisheh M, Onaizi SA. Demulsification of stable emulsions from produced water using a phase separator with inclined parallel arc coalescing plates. J Petrol Sci Eng. 2015; 135: 16-21. https://doi.org/10.1016/j.petrol.2015.08.005

[17] Kim DK, Choi G, Ko T-J, Shin S, Kim SJ. Numerical investigation of oil–water separation on a mesh-type filter. Acta Mech. 2022; 233: 1041-59. https://doi.org/10.1007/s00707-022-03155-0

[18] Yuan S, Fan Y, Li J, Zhou S, Cao Y. Influence of droplet coalescence and breakup on the separation process in wave-plate separators. Can J Chem Eng. 2018; 96: 1627-36. https://doi.org/10.1002/cjce.23089

[19] Oruç M, Yayla S. Experimental investigation of oil-in water separation using corrugated plates and optimization of separation system. Sep Sci Technol. 2022; 57: 788-800. https://doi.org/10.1080/01496395.2021.1939377

[20] Yayla S, Ibrahim SS, Olcay AB. Numerical investigation of coalescing plate system to understand the separation of water and oil in water treatment plant of petroleum industry. Eng Appl Comp Fluid. 2017; 11: 184-92. https://doi.org/10.1080/19942060.2016.1273137

[21] Yayla S, Sabah S, Olcay AB. CFD simulation of designed coalescing plates for separating water and oil in water treatment plants used in petroleum projects. Pamukkale U J Eng Sci. 2017; 23: 358-63. https://doi.org/10.5505/pajes.2016.67944

[22] Liu Y, Lu H, Li Y, Xu H, Pan Z, Dai P, *et al*. A review of treatment technologies for produced water in offshore oil and gas fields. Sci Total Environ. 2021; 775: 145485. https://doi.org/10.1016/j.scitotenv.2021.145485

[23] Wahba E. Derivation of the differential continuity equation in an introductory engineering fluid mechanics course. Int J Mech Eng Edu. 2022; 50: 538-47. https://doi.org/10.1177/03064190211014460

[24] Wang Z-H, Liu X-Y, Zhang H-Q, Wang Y, Xu Y-F, Peng B-L, *et al*. Modeling of kinetic characteristics of alkaline-surfactant-polymer-strengthened foams decay under ultrasonic standing wave. Petrol Sci. 2022; 19: 1825-39. https://doi.org/10.1016/j.petsci.2022.04.012

[25] Wang Z, Sun X, Li J, Zhou N. Influencing factors and laws of polymer-flooding produced water separation settlement with dissolved air flotation. China Petrol Mach. 2020; 48: 123-35. https://doi.org/10.16082/j.cnki.issn.1001-4578.2020.10.019

[26] Zhuge X, Qi X, Wang S, Liu Y. Evaluation and improvement of the performance of a wellhead multistage bundle gas-liquid separator. Processes. 2022; 10(4): 632. https://doi.org/10.3390/pr10040632

[27] Hattori H, Wada A, Yamamoto M, Yokoo H, Yasunaga K, Kanda T, *et al*. Experimental study of laminar-to-turbulent transition in pipe flow. Phys Fluids. 2022; 34: 1-18. https://doi.org/10.1063/5.0082624

[28] Zhao J, Xi X, Dong H, Wang Z, Zhuo Z. Rheo-microscopy in situ synchronous measurement of shearing thinning behaviors of waxy crude oil. Fuel. 2022; 323: 124427. https://doi.org/10.1016/j.fuel.2022.124427

[29] Pavlíček P. Local reynolds number. AIP Conference Proceedings 27 June 2019; 2118(1): 030035. https://doi.org/10.1063/1.5114763

[30] Zhao ZG, Feng MQ, Liu JG, Tao YK, Wang JS, Wang L, *et al*. The research on new technology and separation performance of wastewater treatment for offshore field. Desalin Water Treat. 2018; 125: 116-23. https://doi.org/10.5004/dwt.2018.22093.

[31] Koutsourakis N, Bartzis JG, Markatos NC. Evaluation of Reynolds stress, k-ε and RNG k-ε turbulence models in street canyon flows using various experimental datasets. Environ Fluid Mech. 2012; 12: 379-403. https://doi.org/10.1007/s10652-012-9240-9

[32] Galbraith MC, Caplan PC, Carson HA, Park MA, Balan A, Anderson WK, *et al*. Verification of unstructured grid adaptation components. AIAA J. 2020; 58: 3947-62. https://doi.org/10.2514/1.J058783

[33] Yu H, Zhang H, Guo Y, Tan H, Li Y, Xie G. Investigating neutron back scattering technique for the detection of oil water separation levels in horizontal gravity oil separators. J Radioanal Nucl Ch. 2018; 315: 323-30. https://doi.org/10.1007/s10967-017-5675-2

[34] Feng X, Stewart S, Sartori L, Hodges K. Understanding the effect of skim oil recycle on the water/oil separation in steam assisted gravity drainage operations. J Petrol Sci Eng. 2020; 192: 107233. https://doi.org/10.1016/j.petrol.2020.107233